Wireless Power Transfer

ARTICLE

Open Access

https://doi.org/10.48130/wpt-0024-0011

Wireless Power Transfer **2024**, 11: e011

A special LCC-S compensated WPT system with inherent CC-CV transition for electric bicycles charging

Xuebin Zhou[1*], Yonghong Tan[1], Linhui Wang[1], Aiwu Chen[1] and Lin Yang[2]

[1] *College of Intelligent Manufacturing, Hunan University of Science and Engineering, Yongzhou 425199, China*
[2] *College of Electronic and Electrical Engineering, Henan Normal University, Xinxiang 453007, China*
* Corresponding author, E-mail: zhouxuebin821025@huse.edu.cn

Abstract

The charging algorithm of first constant current (CC) and then constant voltage (CV) is popular for electric bicycle onboard battery packs. This manuscript proposes an LCC-S compensated wireless power transfer (WPT) system to realize inherent CC and CV characteristics and automatic CC-CV transition function. During charging, the proposed system can operate in SS tank for CC charging and LCC-S tank for CV charging, respectively. Unlike the previous closed-loop control, hybrid topology switching, and dual-frequency switching methods, the proposed method has an automatic CC-CV transition function due to the special circuit structure. The detection circuits, communication links, and open-circuit protection circuits are omitted, and the system's receiver conforms to the minimalist design principle. Therefore, the proposed system is low-cost, robust, and simple. A confirmatory experimental prototype is fabricated to verify the correctness and effectiveness of the proposed system.

Citation: Zhou X, Tan Y, Wang L, Chen A, Yang L. 2024. A special LCC-S compensated WPT system with inherent CC-CV transition for electric bicycles charging. *Wireless Power Transfer* 11: e011 https://doi.org/10.48130/wpt-0024-0011

Introduction

Generally, to ensure the high efficiency and safety of charging, the typical charging algorithm of electric bicycle onboard battery packs is first constant current (CC) and then constant voltage (CV). In order to design a WPT system that complies with the above-mentioned charging algorithm, three traditional closed-loop control methods of phase shift control[1–3], frequency conversion control[4–6], and DC–DC assistive control[7–9] are adopted. However, the above three control methods all increase the complexity of the system controller design.

The hybrid topology switching method, is extensively studied for its simplicity of control. Various authors[10–15] propose multiple types of hybrid topologies to realize CC and CV charging characteristics. However, additional passive components, AC switches, and corresponding driving circuits are unavoidable in hybrid topologies, which increases the complexity of the circuit structure.

Nowadays, as an alternative, the dual-frequency switching method is gaining popularity. Previous researchers[16–21] present various types of dual-frequency switching methods to achieve CC and CV charging characteristics. However, since some standard frequency recommendations such as from 79 to 90 kHz in the SAEJ2954 standard from the Society of Automotive Engineers, it is difficult to tune circuit parameters to meet actual application requirements.

In addition, the three methods mentioned above have to rely on additional detection circuits and communication links to determine the timing of CC-CV transition. To prevent the risk of accidental load open-circuit in CC mode, it is essential to add open-circuit protection circuits in the above-mentioned methods. Committed to the further optimization of CC and CV WPT systems, this manuscript proposes an LCC-S compensated WPT system to realize inherent CC and CV characteristics and automatic CC-CV transition function. Complicated control, cumbersome circuit structure, difficult-to-adjust parameters, and expensive detection circuits, communication links, open-circuit protection circuits can be avoided, so the proposed system is robust, simple, and low-cost. The proposed system is preferentially recommended for low and medium-power charging applications such as electric bicycles.

Theoretical analysis

The overall circuit structure of the proposed WPT system is depicted in Fig. 1. This structure can be seen as a cascade of a clamp circuit composed of diodes D_1, D_2, and a special LCC-S compensation WPT system. E is the DC input voltage. For the convenience of analysis, the components in the topology are recorded as L_R, L_S, L_P, C_R, C_P, and C_S respectively. The mutual inductance of L_S and L_P is denoted as M. U_{AO} and U_{BO} are the AC output voltages from the clamp circuit and the half-bridge inverter, respectively. The equivalent AC resistance of the part surrounded by the blue dotted line is expressed as R_E and satisfies the relation $R_E = 2R_B/\pi^2$. There are three operating modes for the clamp circuit: the turned-off mode, the partly activated mode, and the fully active mode, and these three modes correspond to CC mode, CC-CV transition process, and CV mode respectively. The analysis of the different modes is given as follows:

Analysis of CC mode

At the initial stage of charging, since $\sqrt{2}|U_{AO}| \leqslant E$, the clamp circuit is in the turned-off mode and the branch where LR is located is disconnected. The proposed system operates in an SS tank to perform CC charging, as shown in Fig. 2. C_R and C_P can be equivalent to C_{PR}, and the equivalent relationship is $1/C_{PR} = 1/C_P + 1/C_R$. According to Kirchhoff's voltage law (KVL), Eqn (1) can be obtained as:

$$\begin{cases} U_{BO} = \left(j\omega L_P + \dfrac{1}{j\omega C_{PR}}\right) I_2 + j\omega M I_3 \\ 0 = \left(j\omega L_S + \dfrac{1}{j\omega C_S} + R_E\right) I_3 + j\omega M I_2 \end{cases} \tag{1}$$

For simplicity of analysis, it is assumed that all compensation capacitors are fully compensated at a fixed angular frequency ω. The compensation relationships are as follows:

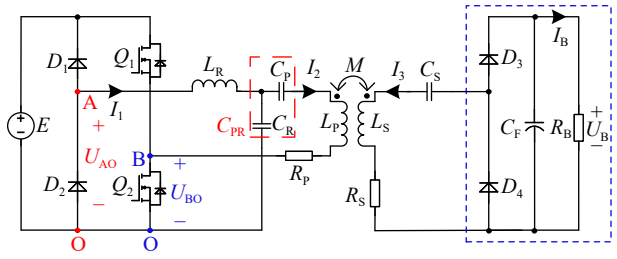

Fig. 1 Overall circuit structure of the proposed WPT system and circuit structure of the WPT system working in CV mode.

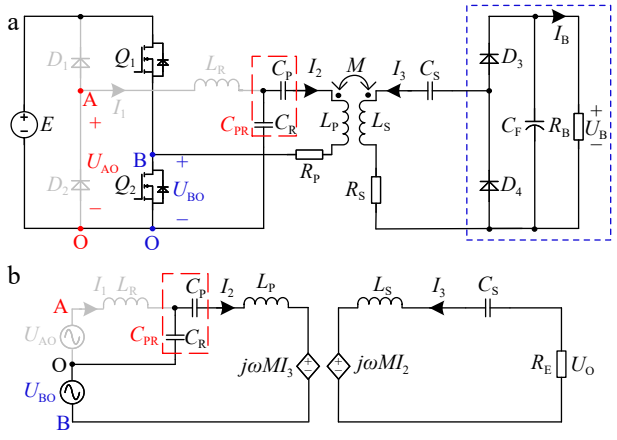

Fig. 2 Circuit structure and equivalent circuit of the WPT system working in CC mode. (a) Circuit structure diagram. (b) Equivalent circuit diagram.

$$j\omega L_P + \frac{1}{j\omega C_{\mathrm{PR}}} = 0,\ j\omega L_{\mathrm{S}} + \frac{1}{j\omega C_{\mathrm{S}}} = 0 \tag{2}$$

Combining Eqns (1) & (2), $R_E = 2R_B/\pi^2$ and $I_B = (\sqrt{2}/\pi)I_3$, Eqn (3) can be derived as:

$$I_B = \frac{2E}{\pi^2\omega M},\ Z_{in} = \frac{U_{BO}}{I_2} = \frac{\omega^2\pi^2M^2}{2R_B^2} \tag{3}$$

It can be known from Eqn (3), the input impedance Z_{in} is purely resistive and the charging current I_{B} is independent of load resistance.

Analysis of CC-CV transition process

When $E \leqslant \sqrt{2}|U_{\mathrm{AO}}| \leqslant (4/\pi)E$, the clamp circuit is in the partly activated mode so that the branch where L_{R} is located is gradually turned on. When $\sqrt{2}|U_{AO}|$ just exceeds E, the current I_1 is very weak and can be ignored. At this time, the system circuit structure is basically consistent with that in CC mode. When $\sqrt{2}|U_{AO}|$ is close to $(4/\pi)E$, the current I_1 is gradually approaching stability and the system circuit structure is basically consistent with that in CV mode.

Analysis of CV mode

With the continuous increase of $\sqrt{2}|U_{AO}|$, when $(4/\pi)E \leqslant \sqrt{2}|U_{AO}|$, the clamp circuit is fully activated. The proposed system operates in LCC-S topology to perform CV charging, as shown in Fig. 1.

For the clamp circuit composed of D_1 and D_2, the relationship between the RMS value of the output voltage U_{AO} and the input voltage E is $U_{AO} = (\sqrt{2}/\pi)E$, while for the half-bridge inverter composed of Q_1 and Q_2, the relationship between the RMS value of the output voltage U_{BO} and the input voltage E is $U_{BO} = (\sqrt{2}/\pi)E$. Therefore, $U_{AO} = U_{BO}$. From the above analysis, it can be concluded that the full conductive clamp circuit in CV mode is connected in parallel with the half-bridge inverter.

The equivalent circuit in CV mode is displayed in Fig. 3. According to KVL, Eqn (4) can be obtained.

$$\begin{cases} U_{AO} = \left(j\omega L_R + \dfrac{1}{j\omega C_R}\right)I_1 - \dfrac{1}{j\omega C_R}I_2 \\ U_{BO} = \left(j\omega L_P + \dfrac{1}{j\omega C_{PR}}\right)I_2 - \dfrac{1}{j\omega C_R}I_1 + j\omega M I_3 \\ 0 = \left(j\omega L_S + \dfrac{1}{j\omega C_S} + R_E\right)I_3 + j\omega M I_2 \end{cases} \tag{4}$$

Similar to the CC analysis process, Eqn (2) and $j\omega L_R + 1/j\omega C_R = 0$ need to be satisfied. Substituting Eqn (2), $U_{AO} = U_{BO}$ and $j\omega L_R + 1/j\omega C_R = 0$ into Eqn (4), Eqn (5) can be deduced as:

$$U_O = -\frac{MU_{AO}}{L_R},\ Z_{in} = \frac{U_{BO}}{I_2} = -\omega L_R \tag{5}$$

where, U_O is the equivalent AC input voltage of the rectifier.

According to $U_O = (\sqrt{2}/\pi)U_B$, $U_{AO} = (\sqrt{2}/\pi)E$, the expression of the charging voltage U_{B} is as follows:

$$U_B = \frac{M}{L_R}E \tag{6}$$

Equations (5) & (6) prove that the system can achieve load-independent CV output and ZPA operation.

Experimental validation

Experimental prototype

Given an electric bicycle battery pack with a nominal voltage of 60 V and a capacity of 10 Ah, an experimental prototype with 2 A/66 V charging outputs was fabricated, as shown in Fig. 4. The operating frequency f was set as 85 kHz and the input DC voltage E as 100 V. According to Eqns $1/C_{PR} = 1/C_P + 1/C_R$, (2), (3), (6) and $j\omega L_R + 1/j\omega C_R = 0$, the parameters of each compensation component can be calculated, as listed in Table 1.

Experimental results

Experimental waveforms for CC mode, CC-CV transition, and CV mode were captured, as shown in Fig. 5. Figure 5a & b show the experimental waveforms in CC mode at R_B = 10 and 15 Ω,

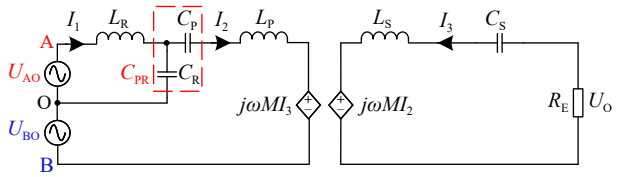

Fig. 3 Equivalent circuit of the WPT system working in CV mode.

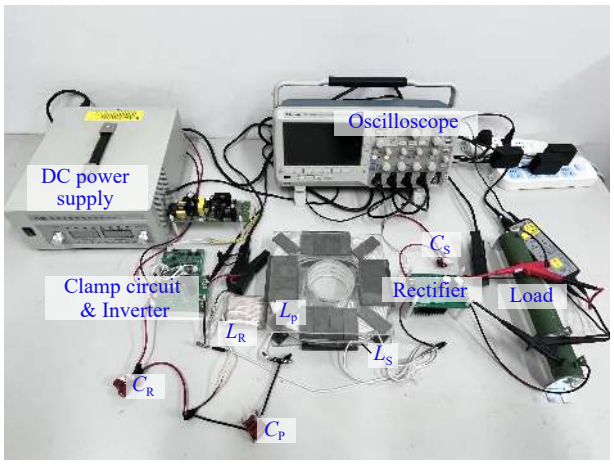

Fig. 4 Experimental prototype.

Table 1. Specific compensation parameters of the proposed system.

Parameters	Value
C_P, C_S, C_R (nF)	175.4, 175.4, 175.4
L_P, L_S, L_R, M (μH)	50, 50, 28.5, 19.2

respectively. I_B maintains at a constant value of 2 A and I_1 is null. Figure 5c & d display that the clamp circuit is partially activated, and the branch where L_2 is located generates discontinuous I_1 during the CC-CV transition process. In CV mode, the clamp circuit is fully activated, the current I_1 is continuous, U_B maintains at a constant value of 66 V and the relevant waveforms are shown in Fig. 5e & f. Furthermore, the phases of the input voltage U_{BO} and the input current I_2 are consistent in the three modes, the proposed system can achieve ZPA operation throughout the charging process.

Figure 6 shows the trends of I_B (represented in red), U_B (represented in blue), and charging efficiency (represented in purple) during the charging process. It can be obtained that when $\sqrt{2}|U_{AO}| \leqslant E$, the system can achieve an approximate CC output of 2 A, while $(4/\pi)E \leqslant \sqrt{2}|U_{AO}|$, the system can achieve an approximate CV output of 66 V. Although the transition from CC to CV mode is not instantaneous, the transition occurs over a fairly short load variation range. Further observation of Fig. 6 shows that the maximum efficiency of the system is 93.3%.

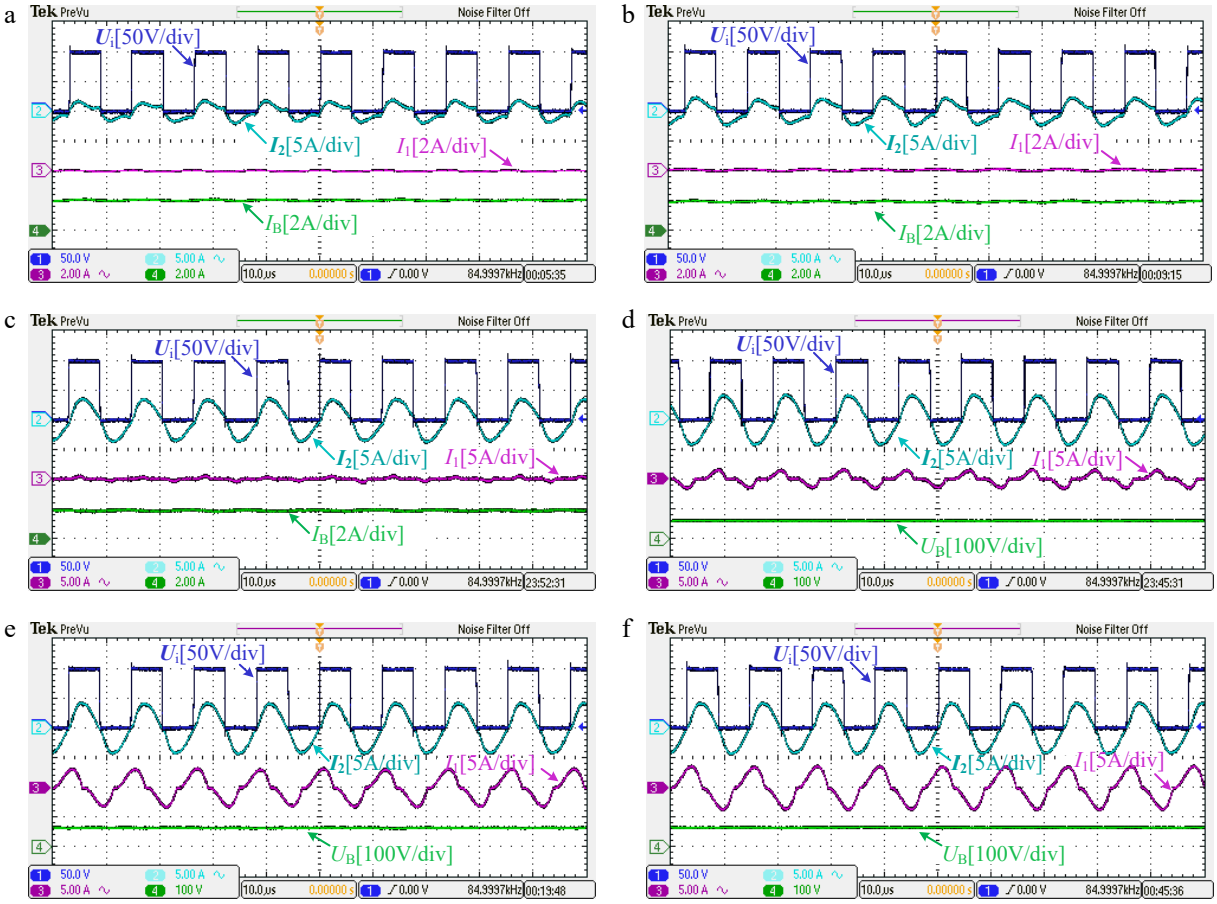

Fig. 5 Experimental waveforms. (a) $R_B = 5\ \Omega$. (b) $R_B = 10\ \Omega$. (c) $R_B = 30\ \Omega$. (d) $R_B = 40\ \Omega$. (e) $R_B = 100\ \Omega$. (f) $R_B = 150\ \Omega$.

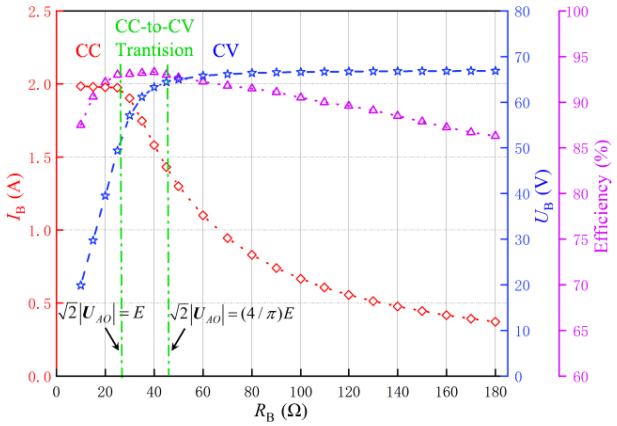

Fig. 6 Measured I_B, U_B, and efficiency curve vs R_B.

Conclusions

The current study proposes a special LCC-S compensated WPT system with inherent CC and CV output characteristics and automatic transition from CC to CV charging mode. In the initial stage of the charging, the CC mode can be realized through the SS structure. As charging proceeds, when the voltage peak on the clamp circuit satisfies $(4/\pi)E \leqslant \sqrt{2}|U_{AO}|$, the system automatically converts to the LCC-S structure to perform CV mode. The proposed system not only avoids complex controller design but also eliminates complex and expensive circuits such as wireless communication links, state-of-charge detection circuits, and open circuit protection circuits. Therefore, the system features easy control, a simple structure, and low cost. The proposed system is a potential and competitive candidate in low and medium-power applications.

Author contributions

The authors confirm contribution to the paper as follows: conceptualization, resources, funding acquisition, writing-original draft preparation, writing-review and editing: Zhou X; methodology, data curation: Zhou X, Tan Y; software: Zhou X, Tan Y, Wang L; validation: Chen A, Yang L; formal analysis: Tan Y, Wang L; Investigation, project administration: Chen A; visualization: Wang L, Chen A; supervision: Yang L. All authors have read and agreed to the final version of the manuscript.

Data availability

All data generated or analyzed during this study are included in this published article.

Acknowledgments

This work was supported in part by the Natural Science Foundation of Hunan Province (Grant No. 2024JJ7186), in part by the Key Laboratory of Small and Micro Intelligent Agricultural Machinery Equipment and Application of Hunan Province Education Department of China (Grant No. SJT012), and in part by the Institute of Image Information Processing and Intelligent Control of Hunan University of Science and Engineering (Grant No. XKY008).

Conflict of interest

The authors declare that they have no conflict of interest.

Dates

Received 13 August 2024; Revised 11 October 2024; Accepted 15 October 2024; Published online 3 December 2024

References

1. Song K, Li Z, Jiang J, Zhu C. 2018. Constant current/voltage charging operation for Series–Series and Series–Parallel compensated wireless power transfer systems employing primary-side controller. *IEEE Transactions on Power Electronics* 33:8065–80
2. Berger A, Agostinelli M, Vesti S, Oliver JA, Cobos JA, et al. 2015. A wireless charging system applying phase-shift and amplitude control to maximize efficiency and extractable power. *IEEE Transactions on Power Electronics* 30:6338–448
3. Colak K, Asa E, Bojarski M, Czarkowski D, Onar OC. 2015. A novel phase shift control of semi-bridgeless active rectifier for wireless power transfer. *IEEE Transactions on Power Electronics* 30:6288–97
4. Liu N, Habetler TG. 2015. Design of a universal inductive charger for multiple electric vehicle models. *IEEE Transactions on Power Electronics* 30:6378–90
5. Zhao Q, Wang A, Liu J, Wang X. 2019. The load estimation and power tracking integrated control strategy for dual-sides controlled LCC compensated wireless charging system. *IEEE Access* 7:75749–61
6. Gati E, Kampitsis G, Manias S. 2017. Variable frequency controller for inductive power transfer in dynamic conditions. *IEEE Transactions on Power Electronics* 32:1684–96
7. Huang Z, Wong SC, Tse CK. 2018. Control design for optimizing efficiency in inductive power transfer systems. *IEEE Transactions on Power Electronics* 33:4523–34
8. Li Z, Zhu C, Jiang J, Song K, Wei G. 2017. A 3-kW wireless power transfer system for sightseeing car supercapacitor charge. *IEEE Transactions on Power Electronics* 32:3301–16
9. Li H, Li J, Wang K, Chen W, Yang X. 2015. A maximum efficiency point tracking control scheme for wireless power transfer systems using magnetic resonant coupling. *IEEE Transactions on Power Electronics* 30:3998–4008
10. Mao X, Chen J, Zhang Y, Dong J. 2022. A simple and reconfigurable wireless power transfer system with constant voltage and constant current charging. *IEEE Transactions on Power Electronics* 37:4921–25
11. Li Y, Hu J, Liu M, Chen Y, Chan KW, et al. 2019. Reconfigurable intermediate resonant circuit based WPT system with load-independent constant output current and voltage for charging battery. *IEEE Transactions on Power Electronics* 34:1988–92
12. Qu X, Han H, Wong SC, Tse CK, Chen W. 2015. Hybrid IPT topologies with constant current or constant voltage output for battery charging applications. *IEEE Transactions on Power Electronics* 30:6329–37
13. Zhang Y, Shen Z, Pan W, Wang H, Wu Y, et al. 2023. Constant current and constant voltage charging of wireless power transfer system based on three-coil structure. *IEEE Transactions on Industrial Electronics* 70:1066–70
14. Mai R, Chen Y, Zhang Y, Yang N, Cao G, et al. 2018. Optimization of the passive components for an S-LCC topology-based WPT system for charging massive electric bicycles. *IEEE Transactions on Industrial Electronics* 65:5497–508
15. Chen Y, Li M, Yang B, Chen S, Li Q, et al. 2020. Variable-parameter T-circuit-based IPT system charging battery with constant current or constant voltage output. *IEEE Transactions on Power Electronics* 35:1672–84
16. Huang Z, Wong SC, Tse CK. 2017. Design of a single-stage inductive-power-transfer converter for efficient EV battery charging. *IEEE Transactions on Vehicular Technology* 66:5808–21
17. Tran DH, Vu VB, Choi W. 2018. Design of a high-efficiency wireless power transfer system with intermediate coils for the OnBoard chargers of electric vehicles. *IEEE Transactions on Power Electronics* 33:175–87
18. Yang L, Li X, Liu S, Xu Z, Cai C. 2021. Analysis and design of an LCCC/S-compensated WPT system with constant output characteristics for battery charging applications. *IEEE Journal of Emerging and Selected Topics in Power Electronics* 9:1169–80
19. Vu VB, Tran DH, Choi W. 2018. Implementation of the constant current and constant voltage charge of inductive power transfer systems with the double-sided LCC compensation topology for electric vehicle battery charge applications. *IEEE Transactions on Power Electronics* 33:7398–410
20. Yang L, Ren L, Shi Y, Wang M, Geng Z. 2023. Analysis and design of an S/S/P-compensated three-coil structure WPT system with constant current and constant voltage output. *IEEE Journal of Emerging and Selected Topics in Power Electronics* 11:2487–500
21. Qu X, Chu H, Wong SC, Tse CK. 2019. An IPT battery charger with near unity power factor and load-independent constant output combating design constraints of input voltage and transformer parameters. *IEEE Transactions on Power Electronics* 34:7719–27